iScience

CellPress
OPEN ACCESS

Article

A triatomic carbon and derived pentacarbides with superstrong mechanical properties

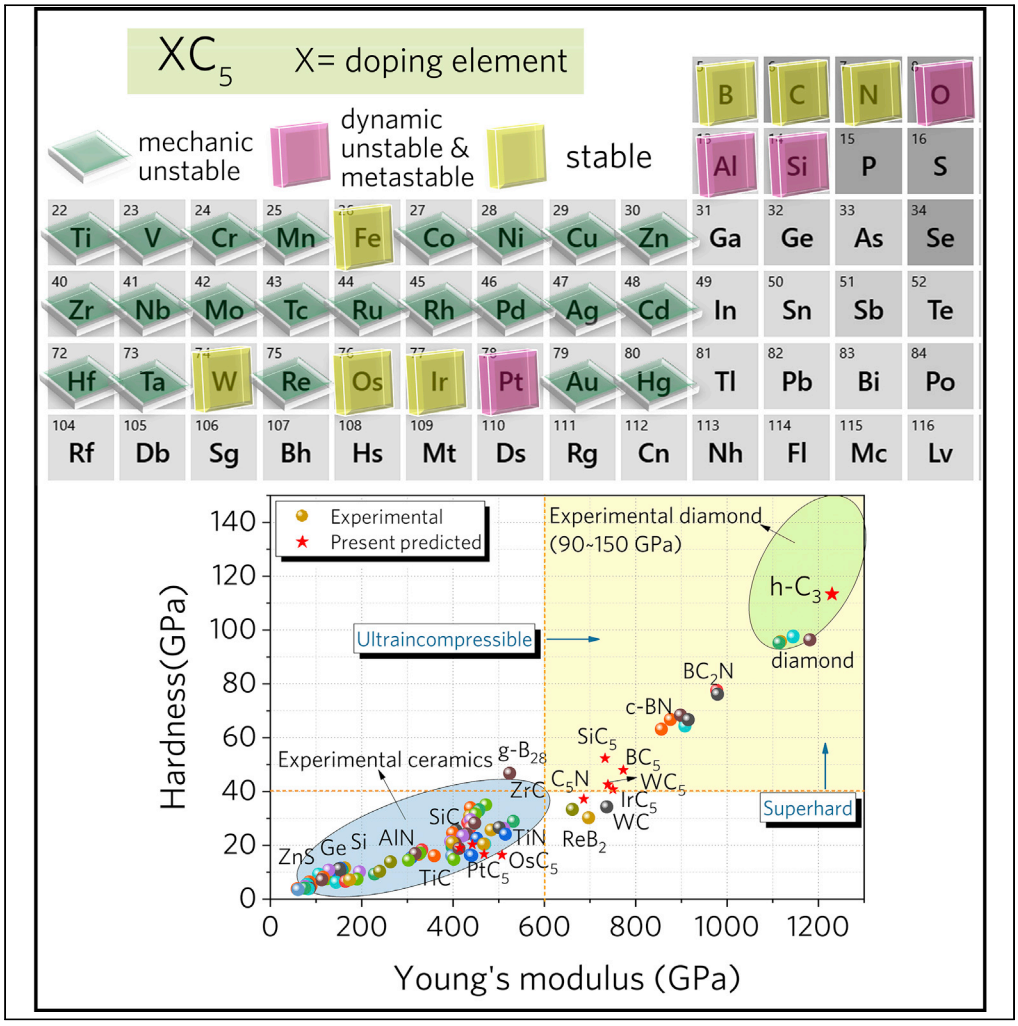

Bingcheng Luo, Longwen Wu, Zili Zhang, Guowu Li, Enke Tian

luobc21@cau.edu.cn (B.L.)
longwen36@scu.edu.cn (L.W.)

Highlights

Stable triatomic carbon allotrope with giant hardness reaching diamond

Structural transformation into two-dimensional carbon monolayer at high temperature

XC_5 (X = Al, Fe, Ir, Os, B, N, Si, W, and O) are strong pentacarbides

SiC_5, BC_5, IrC_5, and WC_5 are superhard materials with Vickers hardness over 40 GPa

Luo et al., iScience 25, 104712
August 19, 2022
https://doi.org/10.1016/j.isci.2022.104712

iScience

CellPress
OPEN ACCESS

Article

A triatomic carbon and derived pentacarbides with superstrong mechanical properties

Bingcheng Luo,[1,5,*] Longwen Wu,[2,*] Zili Zhang,[3] Guowu Li,[4] and Enke Tian[3]

SUMMARY

Diamond has the largest hardness of any natural material with an experimental Vickers hardness value of 90–150 GPa. Here, we reported the stable triatomic carbon allotrope with giant hardness closing that of diamond and a family of pentacarbides with superstrong mechanical properties from the state-of-the-art theoretical calculations. The triatomic carbon allotrope can be transformed into a two-dimensional carbon monolayer at a high temperature. We predicted that the triatomic carbon allotrope holds a hardness of 113.3 GPa, showing the potential capability of cracking diamond. Substitution with Al, Fe, Ir, Os, B, N, Si, W, and O element resulted in strong pentacarbides with Young's modulus of 400–800 GPa. SiC_5, BC_5, IrC_5, and WC_5 are superhard materials with Vickers hardness over 40 GPa, of which BC_5 was successfully synthesized in previous experimental reports. Our results demonstrated the potential of the present strong triatomic carbon and pentacarbides as future high-performance materials.

INTRODUCTION

Carbon, the fourth most abundant element in the universe, has various allotropes due to its sp^1 , sp^2, and sp^3-hybridized bonds. The best-known allotropes are graphite and diamond, representing one of the softest materials and the hardest materials known in the world, respectively. The discoveries of fullerenes (Kroto et al., 1985), carbon nanotubes (Iijima and Ichihashi, 1993), and graphene (Novoselov et al., 2005) have generated intense scientific and technological impacts in relevant fields such as transistors (Wang et al., 2009), photonics (Liu et al., 2011), optoelectronics (Bonaccorso et al., 2010), and energy conversion and storage (Bonaccorso et al., 2015). With the development of synthetic and computational methods, large efforts have been paid to explore novel carbon allotropes. For example, a cold-compression experiment with graphite identified one allotrope of carbon with a hardness hard as diamond (Mao et al., 2003). M-carbon (Li et al., 2009) and bct-C_4 carbon (Umemoto et al., 2010) were predicted to address the unknown structure of cold-compressed graphite, and results showed matched X-ray diffraction (XRD) patterns. Later, W-carbon (Wang et al., 2011), Cco-C_8 carbon (Zhao et al., 2011), and T-carbon (Sheng et al., 2011) were predicted utilizing the first-principles calculations. V-carbon was identified as a monoclinic structure with atoms connected by fully sp^3-hybridized bonds from cold-compressed C_{70} peapods (Yang et al., 2017). Amorphous diamond sp^3-bonded amorphous structure and diamond-like strength were obtained through compressing glassy carbon above 40 GPa (Lin et al., 2011).

Superhard materials include diamond, cubic BN, ReB_2 (Chung et al., 2007), and WB_4 (Mohammadi et al., 2011), usually defined with a Vickers hardness value higher than 40 GPa, are of great interest in many fields such as high-performance cutting tools and wear-resistant and protective coatings (Cook and Bossom, 2000; Wentorf et al., 1980). Among these, diamond is the hardest substance with an experimental Vickers hardness value of 90–150 GPa, which originated from the pyramid-like tetrahedral structure with sp^3-hybridized bond. Polycrystalline diamond can be synthesized from the transformation of graphite at temperatures of 2,300°C–2,500°C and pressures of 12–25 GPa (Irifune et al., 2003). However, the stability of many superhard materials is independent of temperature, pressure, and synthesis methods. Therefore, the rational design of superhard materials requires synergy between theory and experiment (Avery et al., 2019). Using the *ab* initio evolutionary algorithm method, many carbon allotropes, especially superhard carbon phase, have been proposed, including all sp^3-hybridized carbon like M-carbon (Li et al., 2009), W-carbon (Wang et al., 2011), Cco-C_8 carbon (Zhao et al., 2011), and pure sp^2-hybridized carbon such as K_4-carbon (Itoh et al., 2009), Rh_6 (Wang et al., 2014), cT_8 (Lv et al., 2017), and those mixed hybridizations such as orth-C_{10} (Liu et al., 2020), hex-C_{24}, etc. Recent machine-learning-informed evolutionary structure search (Avery et al., 2019) predicted 43 previously unknown forms of superhard carbon phase with Vickers hardness values of 45–80 GPa based on the hardness model (Teter, 2013) (Tian et al., 2012).

[1]College of Science, China Agricultural University, Beijing 100083, China

[2]College of Electrical Engineering, Sichuan University, Chengdu 610065, P. R. China

[3]School of Science, China University of Geosciences, Beijing 100083, China

[4]Crystal Structure Laboratory, National Laboratory of Mineral Materials, China University of Geosciences, Beijing 100083, P. R. China

[5]Lead contact

*Correspondence: luobc21@cau.edu.cn (B.L.), longwen36@scu.edu.cn (L.W.)

https://doi.org/10.1016/j.isci.2022.104712

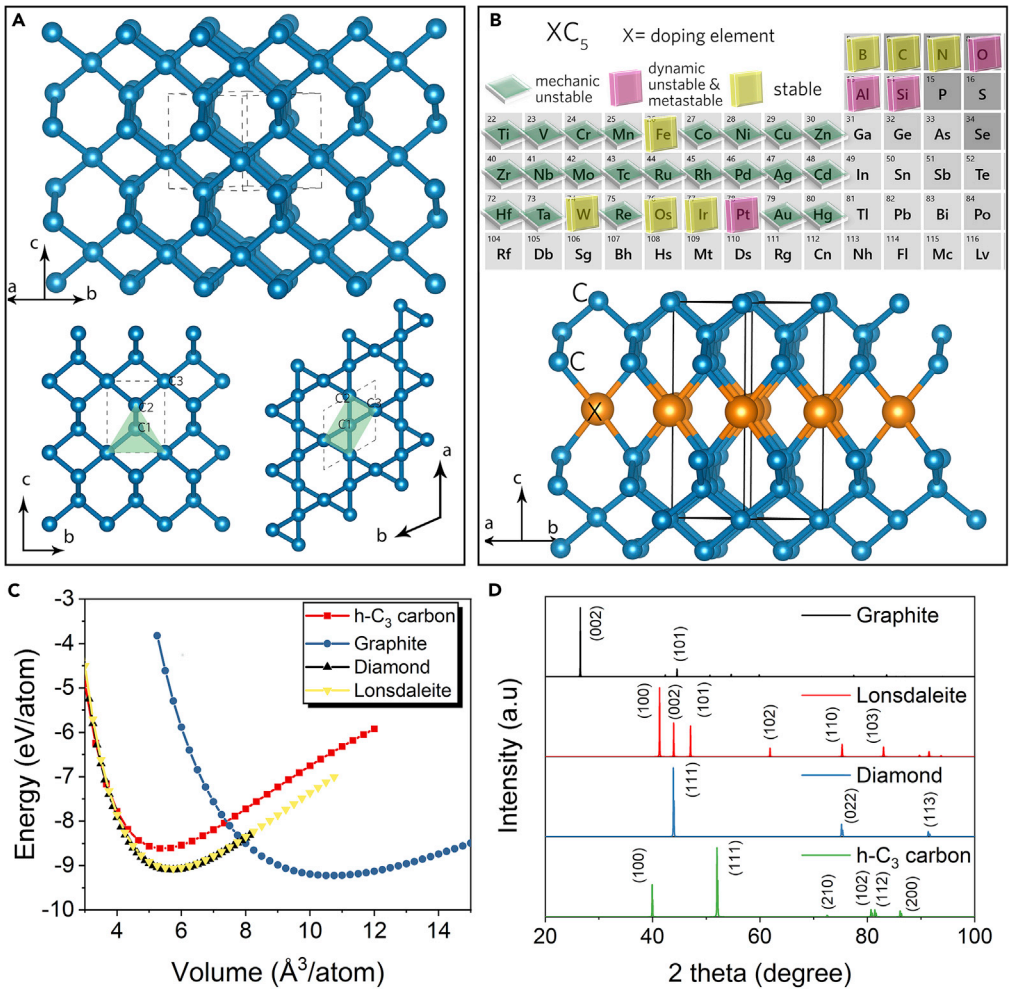

Figure 1. Structural properties of triatomic carbon allotrope and pentacarbides

(A) Crystal structure of triatomic carbon allotrope given three directions with green shades showing the polyhedral unit.

(B) Crystal structure of pentacarbides derived from the substitution of 1/6 triatomic carbon atoms with 32 different elements as shown in the periodic element table.

(C) The total energy per atom of carbon allotropes as a function of volume per atom is calculated from the SCAN- rvv10 exchange functional.

(D) XRD patterns of triatomic carbon allotrope in comparison with diamond, graphite, and lonsdaleite.

In this work, we discovered one triatomic carbon allotropes with giant hardness reaching the hardness of diamond and a family of petancarbides with strong mechanic properties from first-principles calculations (Luo et al., 2019; Lv et al., 2012; Wang et al., 2010). The triatomic carbon allotropes are composed of three atoms per hexagonal unit cell, showing thermal, mechanical, and dynamic stability. We predicted that the h-C_3 holds a hardness of 113.3 GPa, showing the capability of cracking diamond. Furthermore, a family of pentacarbides is discovered by substituting 1/6 of the triatomic carbon atoms with 32 different elements. Substitution with Al, Fe, Ir, Os, B, N, Si, W, and O element resulted in strong pentacarbides with Young's modulus of 400–800 GPa. SiC_5, BC_5, IrC_5, and WC_5 are superhard materials with Vickers hardness over 40 GPa, in which BC_5 was successfully synthesized in previous reports. The electronic, structural, and mechanic properties and stability are studied.

RESULTS AND DISCUSSION

The crystal structure of the triatomic carbon allotrope (h-C_3) is illustrated in Figure 1A. It is crystallized in a hexagonal structure with a space group P6222 and contains three carbon atoms in a primitive cell. At zero pressure, the equilibrium lattice parameters are $a = b = 2.613$ Å, $c = 2.811$ Å, $\alpha = \beta = 90°$, and $\gamma = 120°$. The

3D view in Figure 1A reveals the structural similarity with diamond, where each carbon atom joins four other carbon atoms in regular tetrahedrons. The structural motif of triatomic carbon allotrope was reported to have a binary counterpart in β-quartz SiO_2, which was described as qtz (Avery et al., 2019; Öhrström and O'Keeffe, 2013), hP3 (Ivanovskii, 2013; Zhu et al., 2011), and cinte (Mujica et al., 2015) according to SACADA database (Hoffmann et al., 2016). It is an all-sp^3-hybridized bonding network with the carbon atoms occupying 3*d* (½, ½, −1/6) Wyckoff position. The overlap populations of three carbon-carbon bonds are equal to 0.88. The values of C1-C2, C2-C3, and C1-C3 bond lengths are all identical at 1.60 Å, larger than 1.54 Å of the diamond. Unlike other superhard carbon allotropes such as bct-C4, Z-carbon, 3D *th*-C_{12}, and oC32, the triatomic carbon allotrope contains neither hexa-, tetra-, penta-, nor other types of carbon rings, and this structural diversity leads to differences in mechanical and electronic properties compared to other carbon allotropes. In addition, the primitive cell of both graphene and diamond contains two atoms, while the conventional cell of the cubic diamond and hexagonal diamond contains eight and four atoms, respectively. The present allotrope composed of three atoms enriches the carbon family. A family of 32 pentacarbides is shown in Figure 1B, by substituting 1/6 of the triatomic carbon atoms with Al, Fe, Ir, Os, Pt, B, N, Si, W, and O elements. The bond lengths between doping atoms with the carbon atom of XC_5 (X = Al, Fe, Ir, W, N, and O element) are 2.02, 1.85, 2.15, 2.12, 2.12, 1.47, and 1.31 Å, respectively (Figure S1). The Si-C bond length of SiC_5 in this work is 1.886 Å, which is in the range of other Si-C compounds such as 1.908 Å of *p*-SiC_2, 1.903 Å of *th*-SiC_2 (Kilic and Lee, 2021a), 1.87–1.92 Å of *t*-SiC (Fan et al., 2017), 1.916 Å of *sila*-SiC_2 (Li et al., 2011), and 1.883 Å in *th*-SiC (Kilic and Lee, 2021c). The total energy per atom of carbon allotropes as a function of the volume per atom is obtained using SCAN-rVV10 functional as shown in Figure 1C. The triatomic carbon has a single minimum with a total energy of −8.61 eV/atom, higher than that of the diamond (−9.09 eV/atom) and lonsdaleite (also called hexagonal diamond, −9.06 eV/atom) within SCAN- rVV10 functional. It is more stable than the experimentally synthesized graphdiyne (8.49 eV/atom) (Li et al., 2010) and the theoretically predicted T-graphene (8.41 eV/atom), suggesting a comparable thermodynamical stability. XRD patterns are simulated with a Cu Kα radiation of wavelength λ = 0.154,056 nm to provide more information for experimental observations (Figure 1D). Two sharp peaks at 2θ = 40° and 2θ = 52° are owing to the (100) and (111) diffraction, which is different from diamond where the peaks of (111), (022), and (113) are observed at 2θ = 44°, 75°, and 92°. The peaks of (210), (102), (112), and (200) are negligibly small, similar to graphite which has a sharp peak with large intensity and several small peaks. These features may help identify the triatomic carbon in the experiments. More interestingly, BC_5 was successfully synthesized by using both a laser-heated diamond anvil cell and a large-volume multi-anvil apparatus (Solozhenko et al., 2009).

The dynamic stability is verified by the phonon dispersions from DFPT calculations using norm-conserving pseudopotentials. As shown in Figures 2A and 2B, no imaginary frequencies are observed throughout the whole Brillouin zone at zero pressure, confirming that the predicted allotrope is dynamically stable. The complete phonon spectrum consists of nine normal modes of vibration including three acoustical branches and six optical branches. According to standard group-theoretical analysis, the phonon modes at the Γ point in the Brillouin-zone center have the representations: $\Gamma = A_2 \oplus B_1 \oplus B_2 \oplus E_2 \oplus 2 \times 10^1$, where A_2, B_1, B_2, E_1, and E_2 are the irreducible representation of the symmetry of lattice vibrations. E_1 mode is both Raman and infrared active, while E_2 mode is only Raman active. Based on the Raman and infrared frequencies, the triatomic carbon structure is expected to be identified in further experiments. Moreover, the carbon allotrope can be dynamically stable under a higher pressure of 100 GPa evidenced by the absence of any frequency in Figure 2B. IrC_5 is dynamically stable as shown in Figure 2C. In Figure 1B, the pentacarbides containing Ti, V, Cr, Mn, Co, Ni, Cu, Zn, Zr, Hf, Nb, Ta, Mo, Tc, Re, Ru, Rh, Pd, Ag, Cd, Au, and Hg element are mechanically unstable. The pentacarbides such as C_5O, PtC_5, AlC_5, and SiC_5 are lattice dynamically unstable or metastable, while pentacarbides such as C_5N, BC_5, FeC_5, WC_5, OsC_5, and IrC_5 are mechanically and dynamically stable. The thermal expansion coefficient of triatomic carbon and pentacarbides XC_5 (X = B, Al, Si, Fe, Ir, O, and W) at constant pressure was calculated based on the DFPT and quasi-harmonic approximation (QHA) as shown in Figures 2D and S7. At 300 K, the thermal expansion of h-C_3 is 7.09 ppm/K. C_5N showed a reduced thermal expansion coefficient of 2.45 ppm/K, while IrC_5 and WC_5 displayed increased thermal expansion coefficient of 11.54 ppm/K and 14.84 ppm/K, respectively.

We further examine the thermal stability of the carbon allotrope by using a larger system of 8 × 8×8 supercell containing 1536 atoms based on the classic molecular dynamic (MD) simulation using NPT ensemble as shown in Figure 2E. The energy remains almost intact after heating up to 2000 K for 100 ps with a time step of 1fs, suggesting that triatomic carbon sustains at high temperature after synthesized. In Figure 2 G, at the

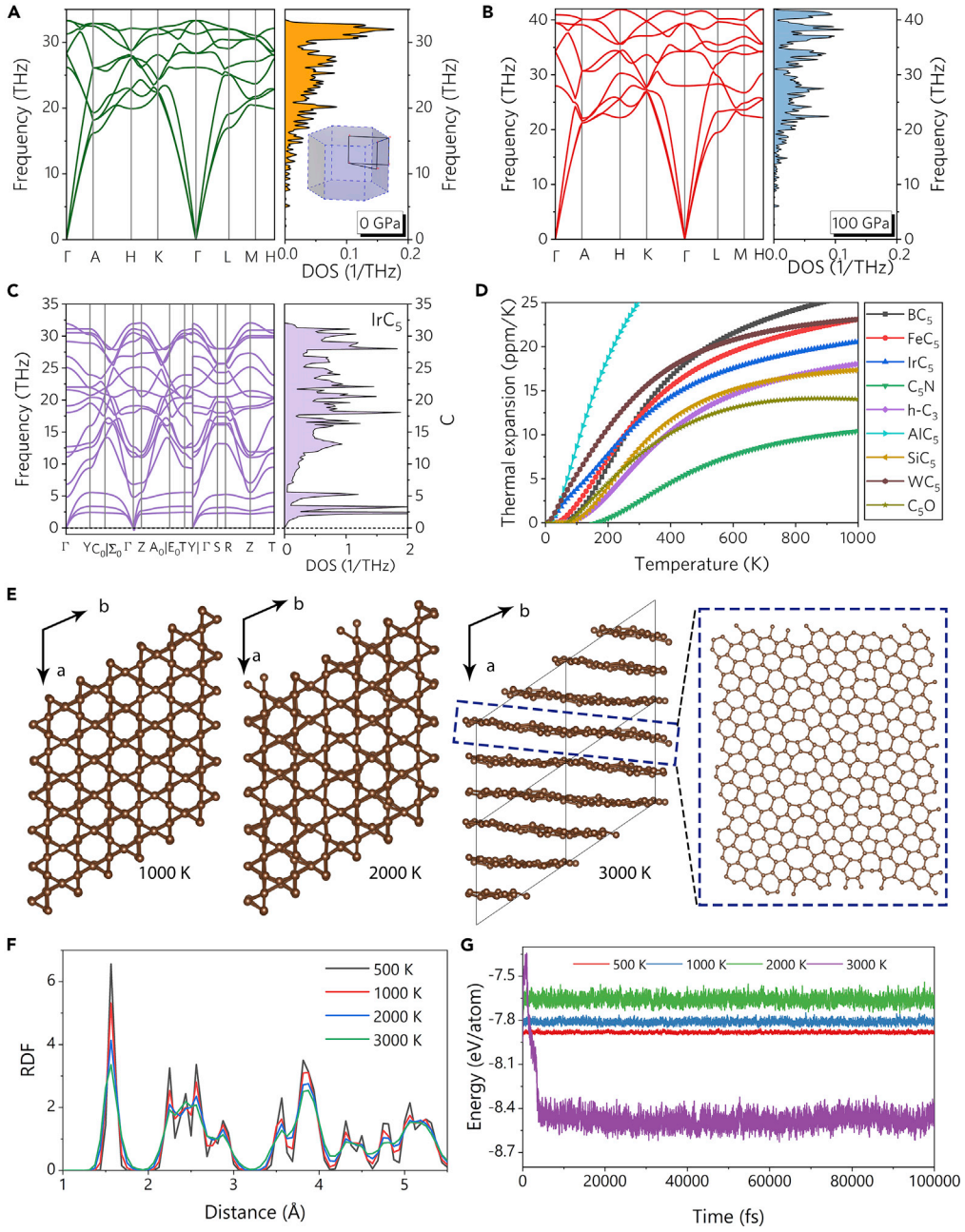

Figure 2. Dynamic stability and thermal stability of triatomic carbon allotropes

(A and B) Phonon dispersion and density of states of the predicted triatomic carbon at the pressure (A) 0 GPa and (B) 100 GPa.

(C) Phonon dispersion and density of states of IrC_5 at 0 GPa.

(D) The volumetric thermal expansion coefficient of triatomic carbon and pentacarbides.

(E) Crystal structures transformation from first-principles molecular dynamic calculations after 100 ps at a given temperature of 1000, 2000, and 3000 K.

(F) Radial distribution function (RDF) of C-C pairs at 1000, 2000, and 3000 K after 100 ps.

(G) Fluctuations of the total energy per atom of triatomic carbon at different temperatures.

temperature of 500, 1000, and 2000 K, the energy difference between the maximum and minimum of energy curves is below 0.2 eV, indicating a small energy fluctuation. However, at an even higher temperature of 3000 K, the structure changed to a new phase which has layered nanosheets as shown in Figures 2E and

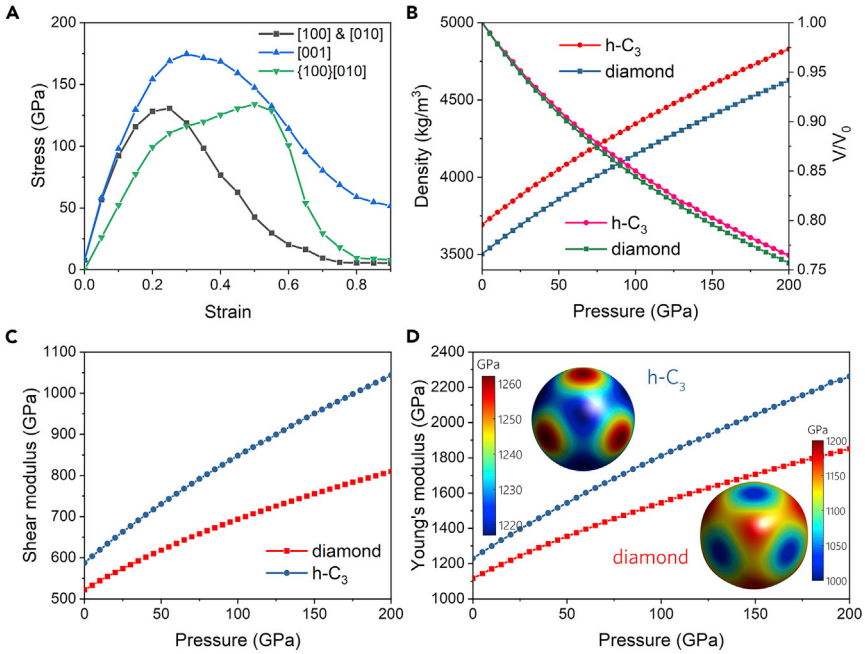

Figure 3. Mechanical properties of triatomic carbon allotrope and pentacarbides

(A) Tensile and shear stress-strain relations along [100], [010], [001], and {100}[010] direction.

(B–D) Density and volume ratio of triatomic carbon and diamond as a function of pressure, (C) Shear modulus of triatomic carbon and diamond as a function of pressure, (D) Young's modulus of triatomic carbon and diamond as a function of pressure, inset showing the corresponding 3D surfaces of Young's modulus.

2G. The new phase of the carbon monolayer sheet is composed of four, five, six, seven, and eight carbon rings in the monoatomic layer. The structural transformation at the high temperature gives hints for the experimental fabrication, which is potential for practical application. In Figure 2F, the first peak of the radial distribution function (RDF) is identical, which is the C-C bond length with a value of 1.60 Å. These further confirm the thermal stability of triatomic carbon for the experimental synthesis.

Figure 3A shows the calculated tensile and shear stress-strain results of triatomic carbon under loading in [100], [010], [001], and {100}[010] direction. Triatomic carbon shows strong stress responses in the [001] direction with a peak tensile strength of 176.2 GPa with a strain of 0.3, which are smaller than 225 GPa of diamond with a strain of 0.4 (Telling et al., 2000). The calculated strengths along the [100], [010], and {100} [010] directions are 121.8 GPa with a strain of 0.2, 121.8 GPa with a strain of 0.2, and 133.9 GPa with a strain of 0.5, respectively, indicating the anisotropy of the tensile strength. The tensile strength of triatomic carbon was comparable to the experimental value of 130 $\pm$ 10 GPa of the in-plane intrinsic tensile strength of monolayer graphene (Lee et al., 2008). To examine the incompressibility of material, the volume compression ratio V/V_0 against hydrostatic pressure is calculated as shown in Figure 3B. With increasing pressure, the volume compression ratio of triatomic carbon decreases, which is slightly larger than that of the diamond. Meanwhile, the density increased with increasing pressure.

The elastic constants are calculated to validate the mechanic stability as listed in Table 1. Results show that elastic constants C_{ij} satisfy the Born stability criteria of the hexagonal system (Mouhat and Coudert, 2014), suggesting that it is mechanically stable at ambient pressure. Large values of C_{11} and C_{33} indicate the strong resistance to linear compression of predicted carbon allotrope along the a, b, and c axis. The calculated average wave velocity of triatomic carbon is 13,721 m/s, higher than 13,283 m/s of the diamond, while the melting temperature of triatomic carbon is 4807 K, higher than 4628 K of the diamond. The calculated bulk modulus B and shear modulus of triatomic carbon from the Voigt-Reuss-Hill (VRH) approximation are 451.6 and 587.2 GPa, respectively, revealing the high incompressibility and shear resistance. Details of calculations are described in STAR Methods. The calculated mechanic properties of the diamond are in good accordance with other theoretical computations and experimental results. As seen in Table 1, the bulk modulus of triatomic carbon is higher than 432.5 GPa of the diamond, whereas the shear modulus of

Table 1. Elastic constants C_{ij}, bulk modulus B, shear modulus G, Young's modulus E, and hardness H of triatomic carbon, together with data for the diamond for comparison

	Triatomic carbon		Diamond			
	This work[a]	This work[b]	This work[a]	This work[b]	Theoretical	Experimental
C_{11}	1268.0	1129.8	1050.5	960.6	1074[c], 1106[d]	1076[e], 1080[f]
C_{12}	82.8	84.0	123.4	76.2	139[c], 141[d]	125[e], 127[f]
C_{44}	563.1	508.6	561.1	506.6	571[c], 607[d]	577[e], 576[f]
C_{13}	26.4	49.2				
C_{33}	1258.3	1123.0				
B	451.6	416.2	432.5	371.0	451[c], 462[d],	442[e], 445[f]
G	587.2	521.1	519.8	480.0	527[c], 545[d]	534[e], 534[f]
E	1229.0	1103.3	1113.4	1006.1	1137[c], 1174[d]	1142[e], 1144[f]
H_v[i]	113.3	99.6	95.7	97.5	92.8[c],96.1[d]	60–120[g], 96 ± 5[h]

The units are GPa.
[a]This work using PAW pseudopotential.
[b]This work using Norm-conserving pseudopotential.
[c]Guo et al. (2020).
[d]Fan et al. (2006).
[e]Grimsditch et al. (Grimsditch and Ramdas, 1975).
[f]Wu et al. (Wu and Wentzcovitch, 2011).
[g]Brazhkin et al. (2004).
[h]Andrievski et al.(Andrievski, 2001).
[i]Tian's model(Tian et al., 2012).

triatomic carbon is higher than 519.8 GPa of the diamond. The ratio of B/G is 0.77, smaller than 0.83 of the diamond, indicating the triatomic carbon allotrope is less brittle than diamond. Young's modulus and Poisson's ratio are defined as the stiffness of materials and the stability of materials under the shear stress. The Young's modulus of h-C_3 is 1229.0 GPa, 10% higher than the value of 1113.4 GPa of the diamond, indicating triatomic carbon is stiffer than that of the diamond. With increasing hydrostatic pressure, the shear modulus and Young's modulus of triatomic carbon and diamond increase obviously, while the values of triatomic carbon are higher than that of diamond as shown in Figures 3C and 3D. The directional dependence of elastic moduli can show the elastic anisotropy of a crystal (Cheng et al., 2014). Analysis of the directional dependence of Young's modulus of triatomic carbon shows that the maximum is 1262 GPa, whereas the minimum is 1217 GPa, even larger than the maximum Young's modulus of 1175 GPa of the diamond as seen in Figure 3D. The ratio of E_{max}/E_{min} for triatomic carbon is 1.04, smaller than 1.15 of the diamond. The universal anisotropy index of H-C_3 and diamond is 0.01 and 0.04, respectively. The average Young's modulus in all directions is 1239 GPa, which is in good agreement with Young's modulus through using VRH approximation. A typical value of Poisson's ratio for metallic materials is 0.33 while the value is 0.1 for covalent materials. The diamond has a strong covalent bond length with a Poisson's ratio of 0.07, and the covalent bond strength of triatomic carbon is 0.04, slightly lower than that of the diamond.

The hardness is calculated according to the model of Mazhnik et al.(Mazhnik and Oganov, 2019, 2020) and Tian et al. (Tian et al., 2012; Xu and Tian, 2015) as shown in Supporting information, which remarkably predicts the hardness and is widely applied in the superhard materials (Avery et al., 2019; He et al., 2018; Sarker et al., 2018; Tian et al., 2013; Zhao et al., 2012). In Figure 4A, the calculated Vickers hardness of triatomic carbon is 113.3 GPa, larger than the values of the diamond using the same methods (Table S1). This is different from the previous literatures (Zhu et al., 2011) in which the Vickers hardness was 87.6 GPa for hP3 lower than 94.3 GPa for diamond. The experimental verification for the Vickers hardness is needed in the future. It is also larger than those of all previous reported superhard materials and carbon allotropes (Avery et al., 2019; Chen et al., 2011; Tian et al., 2012), as seen in Figure 4 and Table S2, including V-carbon of 90 GPa (Yang et al., 2017), M-carbon of 83.1 GPa (Li et al., 2009), Cco-C_8 carbon of 95.1 GPa (Zhao et al., 2011), 4^3T16-CA carbon of 91.16 GPa (Blatov et al., 2021), etc. In Table S1, all the results derived from Tian's model (Tian et al., 2012), Mazhnik's model (Mazhnik and Oganov, 2019, 2020), Chen's model (Chen et al., 2011), and Teter's model (Teter, 2013) showed that h-C_3 is harder than diamond, while Gao's model (Gao et al., 2003) shows that h-C_3 is softer than diamond. In Table 1, the calculated Vickers hardness using the

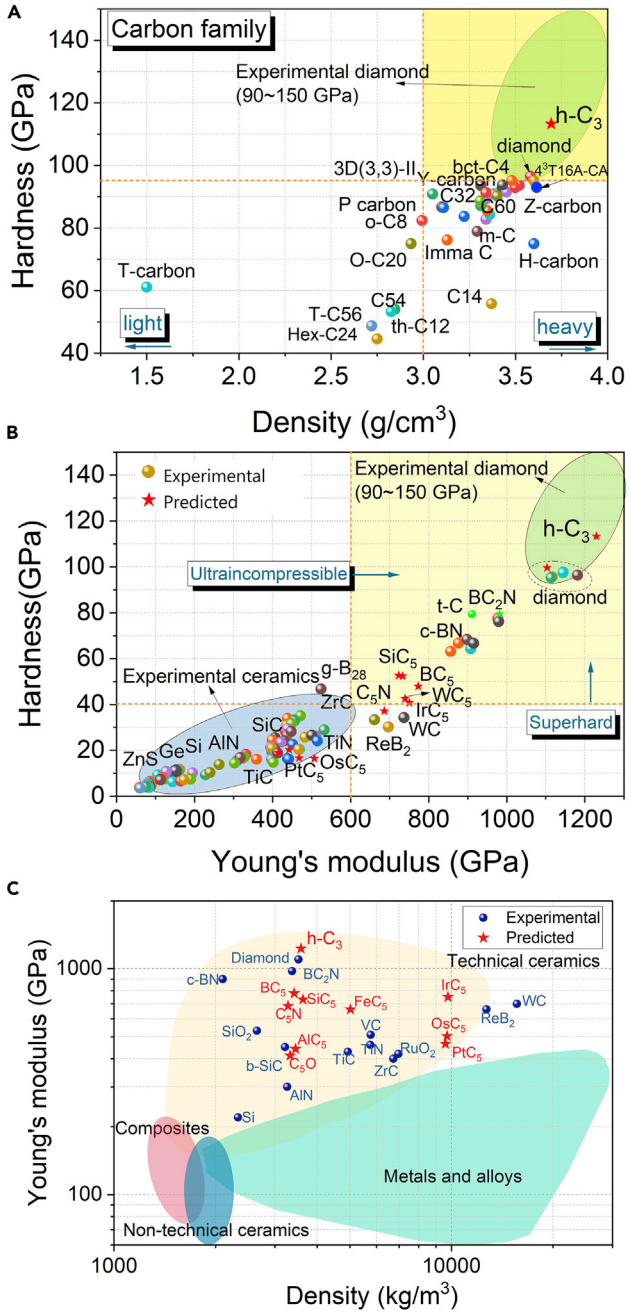

Figure 4. Comparison of mechanical properties of triatomic carbon allotrope and pentacarbides with other materials

(A) Vickers hardness as a function of the density of triatomic carbon with other superhard carbon allotropes.

(B) Comparison of experimental and predicted hardness and Young's modulus of triatomic carbon and pentacarbides with other hard materials.

(C) Chart of Young's modulus as a function of density. The red star depicted the present predicted triatomic carbon and pentacarbides. The experimental hardness of the diamond is 90–150 GPa.

norm-conserving pseudopotential supports the conclusion that h-C_3 is harder. Moreover, the classic MD simulation of a larger system of 15 × 15×15 supercell with 10,125 atoms (Figure S5) using Tersoff forcefield (Tersoff, 1988) shows a Vickers hardness value of 96 GPa from stress-strain calculations, larger than that of the diamond at the same method. In Figures 4B and 4C, substitution with Al, Fe, Ir, Os, B, N, Si, W, and O

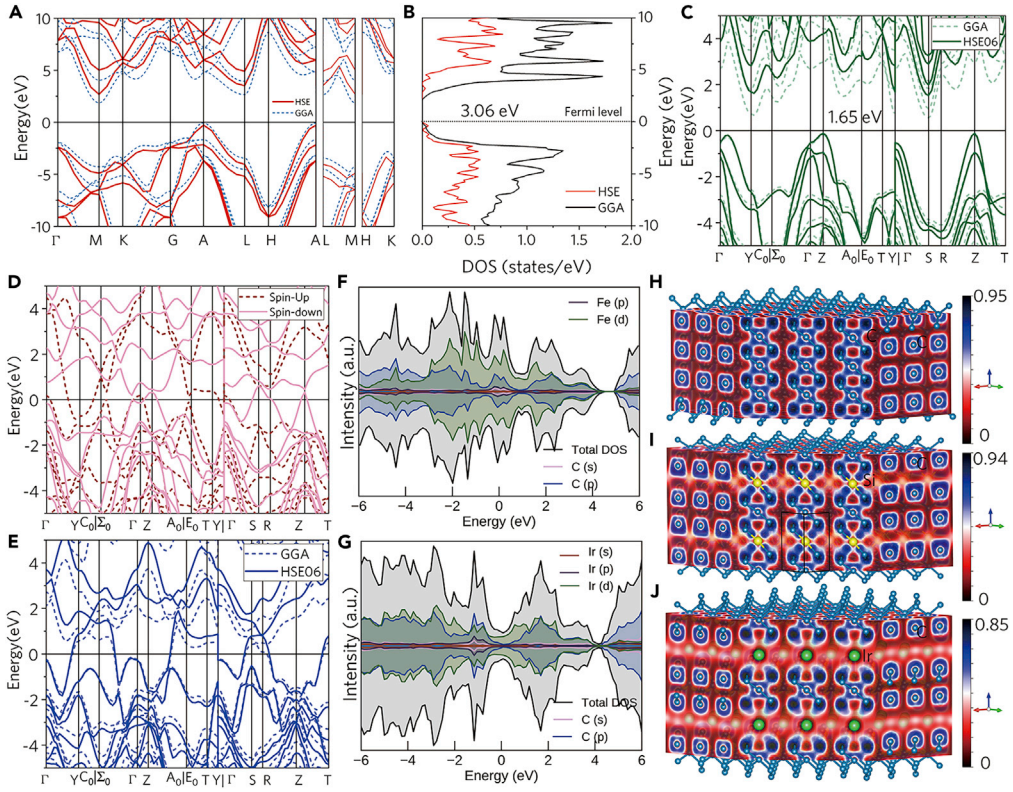

Figure 5. Electronic properties of triatomic carbon allotrope and pentacarbides with other materials

(A) Electronic band structures and (B) density of states (DOS) of triatomic carbon from HSE06 and GGA calculations.
Electronic band structures of (C) SiC_5, (D) FeC_5, and (E) IrC_5.
Total and partial density of states of (F) FeC_5 and (G) IrC_5. Electron localization function of (H) h-C_3, (I) FeC_5, and (J) IrC_5.

element resulted in strong pentacarbides with Young's modulus of 400–800 GPa. For instance, SiC5, IrC_5, and WC_5 showed Young's modulus of 733, 750, and 740 GPa, respectively, which are higher than the common technical ceramics such as AlN, SiO_2, ZrC, TiC, RuO_2, and ReB_2, and larger than the predicted 2D tetrahex carbides(Kilic and Lee, 2021a; c) such as th-SiC, th-GeC, and 2D penta carbides (Kilic and Lee, 2021b) such as p-SiC_2, *p*-GeC_2, and *p*-SnC_2. SiC_5, BC_5, IrC_5, and WC_5 are superhard materials with Vickers hardness of 52.3, 48, 41, and 43 GPa, respectively. Our results demonstrated the potential of the present strong triatomic carbon and pentacarbides as future high-performance materials.

To gain further insights into the chemical bonding and the stabilization mechanisms of triatomic carbon and pentacarbides, the electronic band structure, density of states (DOS), and electron localization function (ELF) are shown in Figure 4. The conduction band minimum (CBM) locates at M point (0.5, 0, 0), and the valence band maximum (VBM) locates at A point (0, 0, 0.5), as seen in Figures 5A and 5B, yielding an indirect semiconductor. It is well known that generalized gradient approximation (GGA) calculations underestimate bandgaps of semiconductors, while the hybrid functionals (HSE) can improve their accuracy for bandgap. HSE06 results showed h-C3 has an insulating feature with an indirect bandgap of 3.06 eV, which is in the range of another carbon allotrope, such as 3.12 eV for Cco-C8 (Zhao et al., 2011), 2.56 eV for bct-C4 (Umemoto et al., 2010), 3.6 eV for M-carbon (Li et al., 2009), and 3.92 eV for th-C12 (Hussain et al., 2022). The SiC_5 allotrope is semiconductors with a bandgap of 1.65 eV using the HSE06 functional (Figure 5C). IrC_5 and FeC_5 are conductors with the crossing of conduction band and valence (Figures 5D and 5E). Analysis of the density of states (Figure S6) shows that the C-2s state mainly contributes to the bands at the lower energy, while the C-2p states account mainly for the valence band and the conduction band region. The contribution of C-2p_z states to the Fermi level is larger than that of C-2p_x and C-2p_y states, whereas the PDOS of C-2p_x and C-2p_y is the same. Obvious orbital hybridization between C-2s and C-2p states is observed as shown in (Figures S2–S4). In pentacarbides, the d-orbital of the transition metal atom is of hybridization with C-2p states (Figures 5F and 5G). ELF is calculated to study the bonding character of

the carbon allotrope (Silvi and Savin, 1994). ELF has values between 0 and 1, where 1 corresponds to perfect localization, namely covalent bonds or lone pairs filled in the core levels; 0.5 corresponds to the electron-gas-like pair probability; and 0 corresponds to no localization, namely the vacuum with no electron density (Tian et al., 2020). From the ELF contours of diamond and triatomic carbon shown in Figures 5H to 5J, the ELF values of the C-C bond for triatomic carbon and diamond are close to 0.90, suggesting the σ-bond covalency of triatomic carbon is as strong as that in the diamond. In IrC_5, weak localization of the Ir-C bond is observed. Analysis of the charge density of triatomic carbon also shows the covalent character of this allotrope. The σ-bonds are formed with all electrons well localized between the C-C atoms, yield to an all-sp^3-hybridized carbon, which is the origin of the superhard properties.

Conclusions

In conclusion, we identified one triatomic carbon allotropes with giant hardness reaching the hardness of diamond and a family of pentacarbides with strong mechanic properties from first-principles calculations. The triatomic carbon is a semiconductor with an indirect bandgap of about 3.06 eV derived from HSE calculations, showing thermal, mechanic, and dynamic stability. The triatomic carbon allotrope can be transformed into a two-dimensional carbon monolayer at a high temperature. We showed the triatomic carbon holds a hardness of 113.3 GPa reaching that of the diamond. Analysis of mechanical properties showed Young's modulus and Vickers hardness are higher than that of the diamond, revealing that the predicted carbon is as hard as diamond. A family of strong pentacarbides with Young's modulus of 400–800 GPa are discovered by substituting 1/6 of the triatomic carbon atoms with Al, Fe, Ir, Os, Pt, B, N, Si, W, and O element. HSE06 bandgap of SiC_5 is 1.65eV, while IrC_5 and FeC_5 are conductors with the crossing of conduction band and valence. SiC_5, BC_5, IrC_5, and WC_5 are superhard materials with Vickers hardness over 40 GPa, in which BC_5 was successfully synthesized in previous reports. The predicted allotrope composed of three carbon atoms would enrich the carbon family and, once synthesized in further experimental studies, will find broad application. Our results demonstrated the potential of the present strong triatomic carbon allotrope and pentacarbides as future high-performance technical ceramics.

Limitations of the study

The theoretical Vickers hardness of carbon allotrope and pentacarbides is derived from the elastic constants using the empirical equations, which inevitably introduces overestimation or underestimation. Even though the empirical equation for predicting the Vickers hardness is widely used, a perfect nonempirical model is needed in the future for a more accurate description of superhard materials. At present, we investigated the carbon allotrope and pentacarbides using theoretical first-principles calculations. Therefore, future experimental verification is needed for lattice structure, stability, and mechanical properties. Typically, the structural characteristic can be further deconstructed using experimental methods such as X-ray diffraction (XRD), scanning tunneling microscopy (STM), and high-resolution transmission electron microscopy (HRTEM). Moreover, we only focused on the XC_5 systems where X = Al, Fe, Ir, Os, Pt, B, N, Si, W, and O elements. There will be a large family of materials holding this type of structure in the combination of other two and more elements, which we will be investigating in the future.

STAR★METHODS

Detailed methods are provided in the online version of this paper and include the following:

- KEY RESOURCES TABLE
- RESOURCE AVAILABILITY
  - Lead contact
  - Materials availability
  - Data and code availability
- EXPERIMENTAL MODEL AND SUBJECT DETAILS
- METHOD DETAILS

SUPPLEMENTAL INFORMATION

Supplemental information can be found online at https://doi.org/10.1016/j.isci.2022.104712.

ACKNOWLEDGMENTS

The authors are grateful for the discussion and suggestions by Prof. Davide M Proserpio and Prof. Kai Xi. This work was supported by the High-performance Computing Platform of China Agricultural University, Scientific Research Start-up Fund for Outstanding Talent (No.10092002 and No. 31051202) of China Agricultural University, Chinese Universities Scientific Fund (No. 15052001), National Natural Science Foundation of China (No. 52002253 and No. 42105056), Sichuan Science and Technology Program (No. 2021YFH0181), and the Fundamental Research Funds for the Central Universities (No. YJ202029). The authors are also grateful for the computational resources provided by Chengdu Supercomputing Center.

AUTHOR CONTRIBUTIONS

B.-C. Luo conceived and performed this study. B.-C. Luo, Z.-L. Zhang, G.-W. Li, and E.-K. Tian performed the data analysis and discussion. B.-C. Luo wrote the first draft of the manuscripts. All authors discussed the results and edited the manuscript.

DECLARATION OF INTERESTS

The authors declare no competing interests.

Received: March 29, 2022
Revised: May 31, 2022
Accepted: June 28, 2022
Published: August 19, 2022

REFERENCES

Andrievski, R.A. (2001). Superhard materials based on nanostructured high-melting point compounds: achievements and perspectives. Int. J. Refract. Metals Hard Mater. *19*, 447–452. https://doi.org/10.1016/s0263-4368(01)00023-3.

Avery, P., Wang, X., Oses, C., Gossett, E., Proserpio, D.M., Toher, C., Curtarolo, S., and Zurek, E. (2019). Predicting superhard materials via a machine learning informed evolutionary structure search. npj Computational Materials *5*, 89. https://doi.org/10.1038/s41524-019-0226-8.

Blatov, V.A., Yang, C., Tang, D., Zeng, Q., Golov, A.A., and Kabanov, A.A. (2021). High-throughput systematic topological generation of low-energy carbon allotropes. npj Comput. Mater. *7*, 15. https://doi.org/10.1038/s41524-021-00491-y.

Bonaccorso, F., Colombo, L., Yu, G., Stoller, M., Tozzini, V., Ferrari, A.C., Ruoff, R.S., and Pellegrini, V. (2015). 2D materials. Graphene, related two-dimensional crystals, and hybrid systems for energy conversion and storage. Science *347*, 1246501. https://doi.org/10.1126/science.1246501.

Bonaccorso, F., Sun, Z., Hasan, T., and Ferrari, A.C. (2010). Graphene photonics and optoelectronics. Nat. Photonics *4*, 611–622. https://doi.org/10.1038/nphoton.2010.186.

Brazhkin, V., Dubrovinskaia, N., Nicol, M., Novikov, N., Riedel, R., Solozhenko, V., and Zhao, Y. (2004). What does 'harder than diamond' mean? Nat. Mater. *3*, 576–577. https://doi.org/10.1038/nmat1196.

Chen, X.-Q., Niu, H., Li, D., and Li, Y. (2011). Modeling hardness of polycrystalline materials and bulk metallic glasses. Intermetallics *19*, 1275–1281. https://doi.org/10.1016/j.intermet.2011.03.026.

Cheng, X.Y., Chen, X.Q., Li, D.Z., and Li, Y.Y. (2014). Computational materials discovery: the case of the W-B system. Acta Crystallogr C Struct. Chem. *70*, 85–103. https://doi.org/10.1107/S2053229613027551.

Chung, H.Y., Weinberger, M.B., Levine, J.B., Kavner, A., Yang, J.M., Tolbert, S.H., Kaner, R.B., and Kaner, R.B. (2007). Synthesis of ultra-incompressible superhard rhenium diboride at ambient pressure. Science *316*, 436–439. https://doi.org/10.1126/science.1139322.

Clark, S.J., Segall, M.D., Pickard, C.J., Hasnip, P.J., Probert, M.I.J., Refson, K., and Payne, M.C. (2005). First principles methods using CASTEP. Zeitschrift für Kristallographie - Crystalline Materials *220*, 567–570. https://doi.org/10.1524/zkri.220.5.567.65075.

Cook, M.W., and Bossom, P.K. (2000). Trends and recent developments in the material manufacture and cutting tool application of polycrystalline diamond and polycrystalline cubic boron nitride. Int. J. Refract. Metals Hard Mater. *18*, 147–152. https://doi.org/10.1016/s0263-4368(00)00015-9.

Fan, C.-Z., Zeng, S.-Y., Li, L.-X., Zhan, Z.-J., Liu, R.-P., Wang, W.-K., Zhang, P., and Yao, Y.-G. (2006). Potential superhard osmium dinitride with fluorite and pyrite structure: first-principles calculations. Phys. Rev. B *74*, 125118. https://doi.org/10.1103/PhysRevB.74.125118.

Fan, D., Lu, S., Guo, Y., and Hu, X. (2017). Novel bonding patterns and optoelectronic properties of the two-dimensional SixCy monolayers. J. Mater. Chem. C *5*, 3561–3567. https://doi.org/10.1039/C6TC05415C.

Gao, F., He, J., Wu, E., Liu, S., Yu, D., Li, D., Zhang, S., and Tian, Y. (2003). Hardness of covalent crystals. Phys. Rev. Lett. *91*, 015502. https://doi.org/10.1103/PhysRevLett.91.015502.

Grimsditch, M.H., and Ramdas, A.K. (1975). Brillouin scattering in diamond. Phys. Rev. B *11*, 3139–3148. https://doi.org/10.1103/PhysRevB.11.3139.

Guo, Y., Cui, L., Zhao, D., Song, T., Cui, X., and Liu, Z. (2020). T-C56: a low-density transparent superhard carbon allotrope assembled from C16 cage-like cluster. J. Phys. Condens. Matter *32*, 165701. https://doi.org/10.1088/1361-648X/ab6710.

He, X.-L., Dong, X., Wu, Q., Zhao, Z., Zhu, Q., Oganov, A.R., Tian, Y., Yu, D., Zhou, X.-F., and Wang, H.-T. (2018). Predicting the ground-state structure of sodium boride. Phys. Rev. B *97*, 100102. https://doi.org/10.1103/PhysRevB.97.100102.

Hoffmann, R., Kabanov, A.A., Golov, A.A., and Proserpio, D.M. (2016). Homo Citans and Carbon Allotropes: For an Ethics of Citation. Angew. Chem. Int. Ed. *55*, 10962–10976. https://doi.org/10.1002/anie.201600655.

Hussain, K., Du, P.H., Mahmood, T., Kawazoe, Y., and Sun, Q. (2022). Three-dimensional tetrahexcarbon: stability and properties. Materials Today Physics *23*, 100628. https://doi.org/10.1016/j.mtphys.2022.100628.

Iijima, S., and Ichihashi, T. (1993). Single-shell carbon nanotubes of 1-nm diameter. Nature *363*, 603–605. https://doi.org/10.1038/363603a0.

Irifune, T., Kurio, A., Sakamoto, S., Inoue, T., and Sumiya, H. (2003). Materials: ultrahard polycrystalline diamond from graphite. Nature *421*, 599–600. https://doi.org/10.1038/421599b.

Itoh, M., Kotani, M., Naito, H., Sunada, T., Kawazoe, Y., and Adschiri, T. (2009). New metallic carbon crystal. Phys. Rev. Lett. *102*, 055703. https://doi.org/10.1103/PhysRevLett.102.055703.

Ivanovskii, A.L. (2013). Search for superhard carbon: between graphite and diamond. J. Superhard Mater. *35*, 1–14. https://doi.org/10.3103/s1063457613010012.

Kilic, M.E., and Lee, K.-R. (2021a). Novel two-dimensional Group-IV carbides containing C2 dimers: sizable direct band gap, high carrier mobility, and anisotropic properties for nanoelectronics. Carbon *181*, 421–432. https://doi.org/10.1016/j.carbon.2021.04.092.

Kilic, M.E., and Lee, K.-R. (2021b). Penta carbides: two-dimensional group-IV semiconductors containing C2 dimers for nanoelectronics and photocatalytic water splitting. Physical Review Materials *5*, 065404. https://doi.org/10.1103/PhysRevMaterials.5.065404.

Kilic, M.E., and Lee, K.-R. (2021c). Tetrahex carbides: two-dimensional group-IV materials for nanoelectronics and photocatalytic water splitting. Carbon *174*, 368–381. https://doi.org/10.1016/j.carbon.2020.12.003.

Kresse, G., and Furthmuller, J. (1996). Efficient iterative schemes for ab initio total-energy calculations using a plane-wave basis set. Phys. Rev. B *54*, 11169–11186. https://doi.org/10.1103/physrevb.54.11169.

Kroto, H.W., Heath, J.R., O'Brien, S.C., Curl, R.F., and Smalley, R.E. (1985). C60: buckminsterfullerene. Nature *318*, 162–163. https://doi.org/10.1038/318162a0.

Lee, C., Wei, X., Kysar, J.W., and Hone, J. (2008). Measurement of the elastic properties and intrinsic strength of monolayer graphene. Science *321*, 385–388. https://doi.org/10.1126/science.1157996.

Li, G., Li, Y., Liu, H., Guo, Y., Li, Y., and Zhu, D. (2010). Architecture of graphdiyne nanoscale films. Chem. Commun. *46*, 3256. https://doi.org/10.1039/B922733D.

Li, Q., Ma, Y., Oganov, A.R., Wang, H., Wang, H., Xu, Y., Cui, T., Mao, H.K., and Zou, G. (2009). Superhard monoclinic polymorph of carbon. Phys. Rev. Lett. *102*, 175506. https://doi.org/10.1103/PhysRevLett.102.175506.

Li, Y., Li, F., Zhou, Z., and Chen, Z. (2011). SiC2 silagraphene and its one-dimensional derivatives: where planar tetracoordinate silicon happens. J. Am. Chem. Soc. *133*, 900–908. https://doi.org/10.1021/ja107711m.

Lin, Y., Zhang, L., Mao, H.K., Chow, P., Xiao, Y., Baldini, M., Shu, J., and Mao, W.L. (2011). Amorphous diamond: a high-pressure superhard carbon allotrope. Phys. Rev. Lett. *107*, 175504. https://doi.org/10.1103/PhysRevLett.107.175504.

Liu, L., Hu, M., Zhao, Z., Pan, Y., and Dong, H. (2020). Superhard conductive orthorhombic carbon polymorphs. Carbon *158*, 546–552. https://doi.org/10.1016/j.carbon.2019.11.024.

Liu, M., Yin, X., Ulin-Avila, E., Geng, B., Zentgraf, T., Ju, L., Wang, F., and Zhang, X. (2011). A graphene-based broadband optical modulator. Nature *474*, 64–67. https://doi.org/10.1038/nature10067.

Luo, B., Yao, Y., Tian, E., Song, H., Wang, X., Li, G., Xi, K., Li, B., Song, H., and Li, L. (2019). Graphene-like monolayer monoxides and monochlorides. Proc. Natl. Acad. Sci. USA *116*, 17213–17218. https://doi.org/10.1073/pnas.1906510116.

Lv, J., Wang, Y., Zhu, L., and Ma, Y. (2012). Particle-swarm structure prediction on clusters. J. Chem. Phys. *137*, 084104. https://doi.org/10.1063/1.4746757.

Lv, Z.-L., Cui, H.-L., Wang, H., Li, X.-H., and Ji, G.-F. (2017). Theoretical study of the elasticity, ideal strength and thermal conductivity of a pure sp^2 carbon. Diam. Relat. Mater. *71*, 73–78. https://doi.org/10.1016/j.diamond.2016.12.005.

Mao, W.L., Mao, H.K., Eng, P.J., Trainor, T.P., Newville, M., Kao, C.C., Heinz, D.L., Shu, J., Meng, Y., and Hemley, R.J. (2003). Bonding changes in compressed superhard graphite. Science *302*, 425–427. https://doi.org/10.1126/science.1089713.

Mazhnik, E., and Oganov, A.R. (2019). A model of hardness and fracture toughness of solids. J. Appl. Phys. *126*, 125109. https://doi.org/10.1063/1.5113622.

Mazhnik, E., and Oganov, A.R. (2020). Application of machine learning methods for predicting new superhard materials. J. Appl. Phys. *128*, 075102. https://doi.org/10.1063/5.0012055.

Mohammadi, R., Lech, A.T., Xie, M., Weaver, B.E., Yeung, M.T., Tolbert, S.H., and Kaner, R.B. (2011). Tungsten tetraboride, an inexpensive superhard material. Proc. Natl. Acad. Sci. USA. *108*, 10958–10962. https://doi.org/10.1073/pnas.1102636108.

Mouhat, F., and Coudert, F.-X. (2014). Necessary and sufficient elastic stability conditions in various crystal systems. Phys. Rev. B *90*, 224104. https://doi.org/10.1103/PhysRevB.90.224104.

Mujica, A., Pickard, C.J., and Needs, R.J. (2015). Low-energy tetrahedral polymorphs of carbon, silicon, and germanium. Phys. Rev. B *91*, 214104. https://doi.org/10.1103/PhysRevB.91.214104.

Novoselov, K.S., Geim, A.K., Morozov, S.V., Jiang, D., Katsnelson, M.I., Grigorieva, I.V., Dubonos, S.V., and Firsov, A.A. (2005). Two-dimensional gas of massless Dirac fermions in graphene. Nature *438*, 197–200. https://doi.org/10.1038/nature04233.

Öhrström, L., and O'Keeffe, M. (2013). Network topology approach to new allotropes of the group 14 elements. Zeitschrift für Kristallographie - Crystalline Materials *228*, 343–346. https://doi.org/10.1524/zkri.2013.1620.

Sarker, P., Harrington, T., Toher, C., Oses, C., Samiee, M., Maria, J.-P., Brenner, D.W., Vecchio, K.S., and Curtarolo, S. (2018). High-entropy high-hardness metal carbides discovered by entropy descriptors. Nat. Commun. *9*, 4980. https://doi.org/10.1038/s41467-018-07160-7.

Sheng, X.L., Yan, Q.B., Ye, F., Zheng, Q.R., and Su, G. (2011). T-carbon: a novel carbon allotrope. Phys. Rev. Lett. *106*, 155703. https://doi.org/10.1103/PhysRevLett.106.155703.

Silvi, B., and Savin, A. (1994). Classification of chemical bonds based on topological analysis of electron localization functions. Nature *371*, 683–686. https://doi.org/10.1038/371683a0.

Solozhenko, V.L., Kurakevych, O.O., Andrault, D., Le Godec, Y., and Mezouar, M. (2009). Ultimate Metastable Solubility of Boron in Diamond: Synthesis of Superhard Diamond like BC_5 Ultimate metastable solubility of boron in diamond: synthesis of superhard Diamond like BC_5. Phys. Rev. Lett. *102*, 015506. https://doi.org/10.1103/PhysRevLett.102.015506.

Telling, R.H., Pickard, C.J., Payne, M.C., and Field, J.E. (2000). Theoretical strength and cleavage of diamond. Phys. Rev. Lett. *84*, 5160–5163. https://doi.org/10.1103/PhysRevLett.84.5160.

Tersoff, J. (1988). New empirical approach for the structure and energy of covalent systems. Phys. Rev. B *37*, 6991–7000. https://doi.org/10.1103/physrevb.37.6991.

Teter, D.M. (2013). Computational alchemy: the search for new superhard materials. MRS Bull. *23*, 22–27. https://doi.org/10.1557/s0883769400031420.

Tian, E., Yao, Y., Luo, B., Niu, Y., Song, H., Li, B., and Song, H. (2020). Tailoring the dimension of halide perovskites enables quantum wires with enhanced visible light absorption. J. Phys. Chem. C *124*, 11124–11131. https://doi.org/10.1021/acs.jpcc.9b11544.

Thompson, A.P., Aktulga, H.M., Berger, R., Bolintineanu, D.S., Brown, W.M., Crozier, P.S., in 't Veld, P.J., Kohlmeyer, A., Moore, S.G., Nguyen, T.D., et al. (2022). LAMMPS - a flexible simulation tool for particle-based materials modeling at the atomic, meso, and continuum scales. Comput. Phys. Commun. *271*, 108171. https://doi.org/10.1016/j.cpc.2021.108171.

Tian, Y., Xu, B., Yu, D., Ma, Y., Wang, Y., Jiang, Y., Hu, W., Tang, C., Gao, Y., Luo, K., et al. (2013). Ultrahard nanotwinned cubic boron nitride. Nature *493*, 385–388. https://doi.org/10.1038/nature11728.

Tian, Y., Xu, B., and Zhao, Z. (2012). Microscopic theory of hardness and design of novel superhard crystals. Int. J. Refract. Metals Hard Mater. *33*, 93–106. https://doi.org/10.1016/j.ijrmhm.2012.02.021.

Umemoto, K., Wentzcovitch, R.M., Saito, S., and Miyake, T. (2010). Body-centered Tetragonal C4: a Viable sp3 Carbon allotrope. Phys. Rev. Lett. *104*, 125504. https://doi.org/10.1103/PhysRevLett.104.125504.

Wang, J.T., Chen, C., and Kawazoe, Y. (2011). Low-temperature phase transformation from graphite to sp3 orthorhombic carbon. Phys. Rev. Lett. *106*, 075501. https://doi.org/10.1103/PhysRevLett.106.075501.

Wang, J.T., Chen, C., Wang, E., and Kawazoe, Y. (2014). A new carbon allotrope with six-fold helical chains in all-sp2 bonding networks. Sci. Rep. *4*, 4339. https://doi.org/10.1038/srep04339.

Wang, X., Li, X., Zhang, L., Yoon, Y., Weber, P.K., Wang, H., Guo, J., and Dai, H. (2009). N-doping of graphene through electrothermal reactions with ammonia. Science *324*, 768–771. https://doi.org/10.1126/science.1170335.

Wang, Y., Lv, J., Zhu, L., and Ma, Y. (2010). Crystal structure prediction via particle-swarm optimization. Phys. Rev. B *82*, 094116. https://doi.org/10.1103/PhysRevB.82.094116.

Wentorf, R.H., Devries, R.C., and Bundy, F.P. (1980). Sintered superhard materials. Science *208*, 873–880. https://doi.org/10.1126/science.208.4446.873.

Wu, Z., and Wentzcovitch, R.M. (2011). Quasiharmonic thermal elasticity of crystals: an analytical approach. Phys. Rev. B *83*, 184115. https://doi.org/10.1103/PhysRevB.83.184115.

Xu, B., and Tian, Y. (2015). Superhard materials: recent research progress and prospects. Science China Materials *58*, 132–142. https://doi.org/10.1007/s40843-015-0026-5.

Yang, X., Yao, M., Wu, X., Liu, S., Chen, S., Yang, K., Liu, R., Cui, T., Sundqvist, B., and Liu, B. (2017). Novel superhard sp3 carbon allotrope from cold-compressed C70 peapods. Phys. Rev. Lett. *118*, 245701. https://doi.org/10.1103/PhysRevLett.118.245701.

Zhao, Z., Tian, F., Dong, X., Li, Q., Wang, Q., Wang, H., Zhong, X., Xu, B., Yu, D., He, J., et al. (2012). Tetragonal allotrope of group 14 elements. J. Am. Chem. Soc. *134*, 12362–12365. https://doi.org/10.1021/ja304380p.

Zhao, Z., Xu, B., Zhou, X.F., Wang, L.M., Wen, B., He, J., Liu, Z., Wang, H.T., and Tian, Y. (2011). Novel superhard carbon: C-centered OrthorhombicC8. Phys. Rev. Lett. *107*, 215502. https://doi.org/10.1103/PhysRevLett.107.215502.

Zhu, Q., Oganov, A.R., Salvadó, M.A., Pertierra, P., and Lyakhov, A.O. (2011). Denser than diamond: Ab initio search for superdense carbon allotropes. Phys. Rev. B *83*. https://doi.org/10.1103/PhysRevB.83.193410.

STAR★METHODS

KEY RESOURCES TABLE

REAGENT or RESOURCE	SOURCE	IDENTIFIER
Software and algorithms		
VASP5	Kresse and Furthmuller, 1996	https://vasp.at/
LAMMPS	Thompson et al., 2022	https://www.lammps.org/
MedeA	Materials Design	https://www.materialsdesign.com/
CASTEP	Clark et al., 2005	http://www.castep.org/
CALYPSO	Wang et al., 2010	http://www.calypso.cn/

RESOURCE AVAILABILITY

Lead contact

Further information and requests should be directed to and will be fulfilled by the lead contact, Bingcheng Luo (luobc21@cau.edu.cn).

Materials availability

This study did not generate any unique reagents.

Data and code availability

- Data reported in this paper will be shared by the lead contact upon request.
- This paper does not report original codes.
- Any additional information required to reanalyze the data reported in this paper is available from the lead contact upon request.

EXPERIMENTAL MODEL AND SUBJECT DETAILS

Our study does not use experimental models typical in the life sciences.

METHOD DETAILS

All methods can be found in the accompanying Transparent Methods supplemental file.